

# ASSESSMENT OF HYDROCARBON CONTAMINATION USING 2D RESISTIVITY IMAGING METHOD AND GEOCHEMICAL ANALYSIS IN IBADAN SOUTHWESTERN, NIGERIA.

## ABSTRACT

2D resistivity imaging survey and geochemical analysis to map and assess the level of soil contamination due to hydrocarbon spillage in Araromi Auto Spare Parts Market Ibadan, Southwestern Nigeria. The objectives are to provide 2D inverted resistivity sections beneath the study area, delineate anomalously low resistivity zones indicative long-term hydrocarbon contamination in the sections, and determine concentrations of Polycyclic Aromatic Hydrocarbons (PAHs) in the suspected soils.

Five traverse were traversed using Wenner array with electrode spacing varied from 5 m to 15 m and station increment of 5 m. The resistivity data were processed by using 2D inversion procedure to generate the 2D inverted resistivity sections. Geochemical analysis was conducted on five soil samples collected at 1 m depth in the low resistivity zones delineated on the 2D inversion sections, to determine the concentration of Polycyclic Aromatic Hydrocarbons (PAHs) to assess the level of contamination.

The 2D inverted sections delineated low resistivity anomalies, ranging from 1.25Ωm to 5.54Ωm, characteristic of mature biodegraded hydrocarbon contamination. The results of geochemical analysis revealed total PAH concentration of 1390 µg/kg to 16140 µg/kg suggesting that the study area is highly contaminated by the used motor oil.

The combined use of 2D resistivity imaging and geochemical analysis has shown that soils beneath the study area has been highly contaminated by the used motor oil, and may constitute potential health risk to the soil and groundwater systems in its vicinity. The results are expected to serve as usefully guide in planning remediation programme.

Keywords: hydrocarbon contamination, resistivity imaging, geochemical analysis, polycyclic aromatic hydrocarbons

Content **Nature terms of use**

## INTRODUCTION

Indiscriminate disposal of used hydrocarbons/used motor oil into the environment from industrial sites is a serious cause for concern as they negatively impact soil and groundwater systems and constitute potential health risk to human population mainly due to the polycyclic hydrocarbons (PAHs) contained in them (Adenijiet *al.*, 2019, Omole *et al.*, 2021, Sun *et al.*, 2021, Faboya *et al.*, 2023).

PAHs are a class of hazardous organic compounds made up of two or more benzene rings in linear, angular, or cluster forms (Balmer *et al.*, 2019, Eldos *et al.*, 2020). They are ubiquitous pollutants, found as mixtures of different chemical compounds, that are discharged into the environment from anthropogenic sources activities mostly incomplete combustion of fossil fuels.

When waste oil seeps into the ground, the PAHs cling to the soil particles in the topsoil and later roam vertically and laterally with rain water that percolates from the surface. Migration of PAHs through soil is usually slow because they do not dissolve easily in water. They are biodegraded by microorganisms after a period of maturity ranging from 4 months to 1 year in soil, releasing by-products which flow with water to form contamination plumes along their paths within the soil and subsequently contaminate the groundwater.

Investigation of hydrocarbon-impacted site is important since contamination of the topsoil would eventually reach the entire subsurface strata and groundwater resources in a matter of time. The speed of migration of the contaminants depends on the prevailing geologic conditions of the soil and the underlying rock.

The traditional techniques for assessing soil contamination and pollution are drilling, sampling and geochemical analysis to determine the concentrations of the chemical constituents of the contaminants. These techniques are, however, point specific and can only reflect scattered local information. They are also invasive, expensive and time-consuming.

Geophysical surveys can provide continuous subsurface information in hydrocarbon-contaminated areas, and have more advantages in being non-invasive and cheaper compared to drilling and sampling (Bertolla *et al.*, 2014; Power *et al.*, 2015; Simyrdanis *et al.*, 2018). Fresh hydrocarbon spills manifest as high resistivity anomalies in resistivity sections (Rosales *et al.*, 2014). Biodegradation of mature hydrocarbon plumes undergoes results in increased total dissolved solids (TDS) and consequent decrease in resistivity presented as low resistivity anomalies (Arato *et al.*, 2014, Subba and Chandrashekhar, 2014, Koroma *et al.*, 2015).

Electrical resistivity tomography (ERT) is widely used in the characterization of hydrocarbon-contaminated sites to detect and delineate contamination plumes and determine to which extent the soil and groundwater have been affected (Orlando and Renzi, 2015, Oyinkuro & Wariebi, 2017, Abbas *et al.*, 2018, Delgado-Rodríguez, *et al.*, 2018). The technique relies on the resistivity

contrast between the contaminated zone and the background geologic 'clean' zone (Akinrinade *et al.*, 2016, Ehirim *et al.*, 2016, Caterina *et al.*, 2017). It is capable of delineating linear geologic features, such as fractures and faults which can serve as conduit for the downward migration of contaminants into the aquiferous units (Al-Menshed and Thabit, 2016, Eze *et al.*, 2021). An integration of geophysical techniques with geochemical data can provide a reliable assessment of the areal extent and level of hydrocarbon contamination (Arato *et al.*, 2014, Azahar *et al.*, 2018, Ciampi *et al.*, 2022).

Used hydrocarbons have been indiscriminately poured on the ground at Araromi Auto Spare Parts Market located at Agodi gate, Ibadan southwestern Nigeria, for over five decades, as old motor parts are disassembled to find reusable parts for sales to prospective buyers. The engine oil wastes are left in contact with the topsoil in which it clings to the surface of soil particles and subsequently migrate with surface/rain water to nearby aquifer units. Assessment of the extent of contamination within and around the location is thus important considering the hazardous effects which the contaminants may have on the soil and groundwater. The findings of the assessment may provide clues for appropriate remediation.

The aim of the study is to carry out 2D resistivity imaging survey and geochemical analysis to map and evaluate the level of soil contamination due to hydrocarbon in Araromi Auto Spare Parts Market Ibadan, Southwestern Nigeria. The objectives are to provide 2D inverted resistivity sections beneath the study area, delineate anomalously low resistivity zones indicative long-term hydrocarbon contamination in the sections, and determine concentrations of Polycyclic Aromatic Hydrocarbons (PAHs) in the suspected soils using geochemical analysis.

The study area is located within latitude  $3^{\circ} 55' 12''\text{N}$  -  $3^{\circ} 55' 19''\text{N}$  and longitude  $7^{\circ} 23' 37''\text{E}$  -  $7^{\circ} 23' 44''\text{E}$  (Fig. 1). Its climate is tropical with distinct wet and dry seasons and a mean annual temperature of  $27.1^{\circ}\text{C}$  (Egbinola and Amanambu, 2013). The rainy season occurs between March and October, when the moist maritime southwest monsoon winds blow inland from the Atlantic

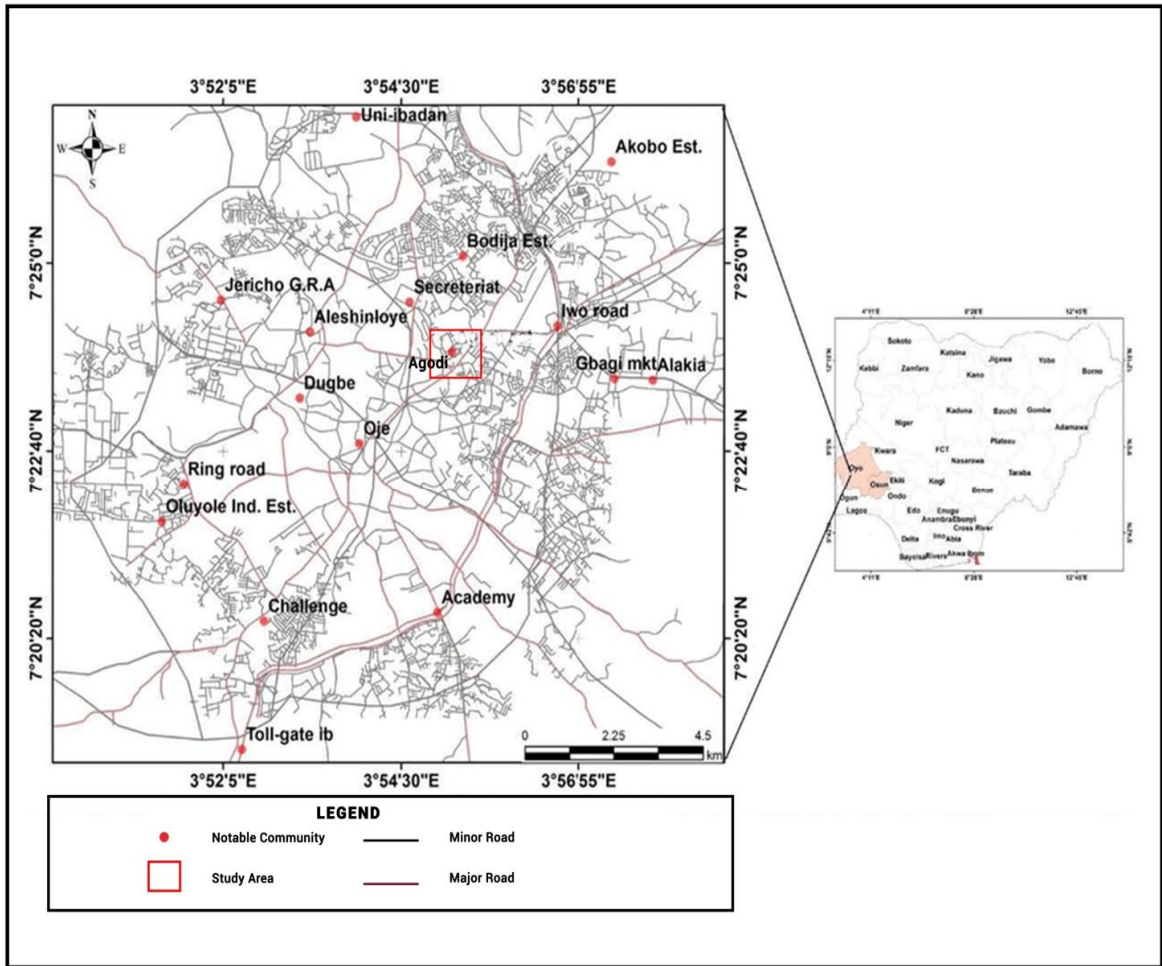
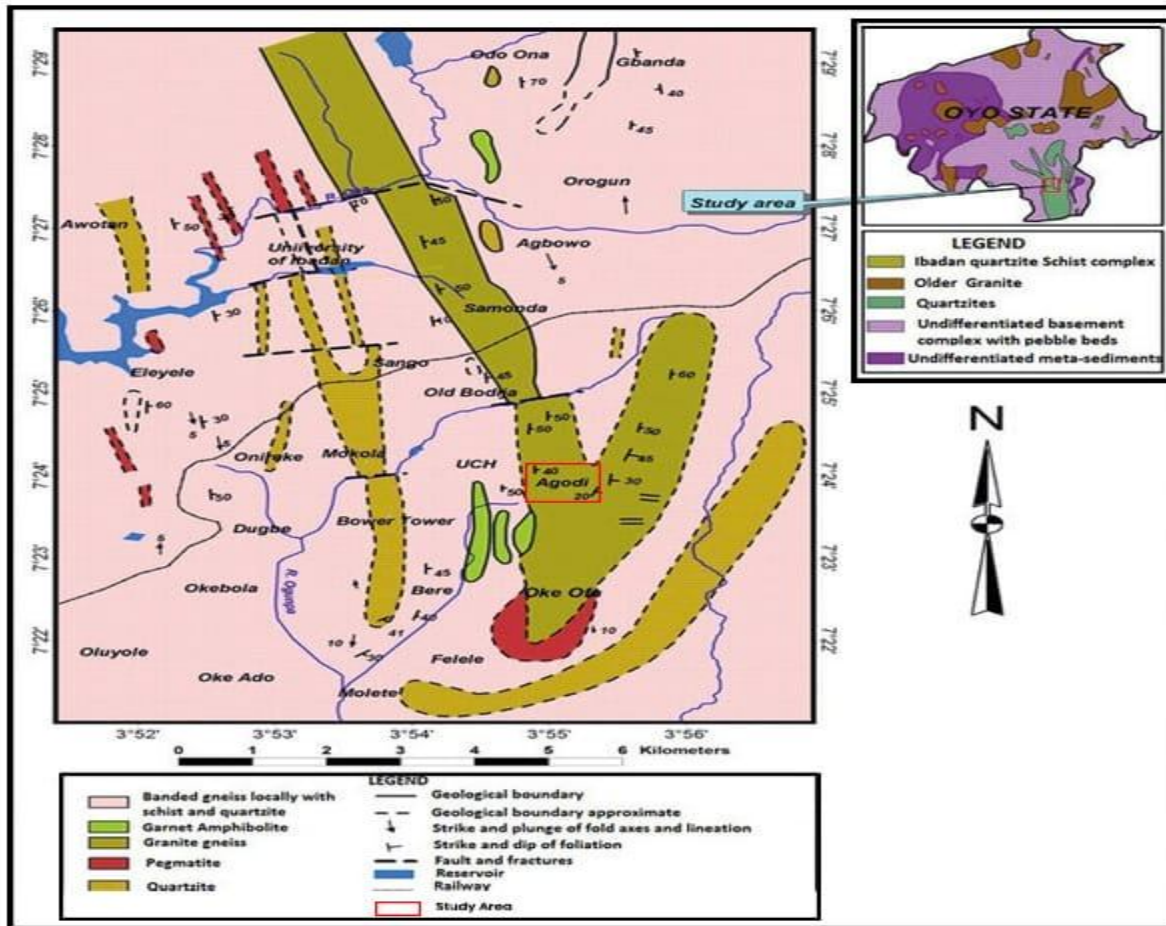


Fig.1: Location map showing the study area



**Fig. 2: Geological map showing the study area**

Ocean, while the dry season occurs from November to February when the dry dust-laden winds blow from the Sahara Desert.

The underlying geology is granite gneiss, a Precambrian basement complex rocks of metamorphic origin (Fig..2). Granite gneiss is a metamorphic rock formed by changing schist, granite, or volcanic rocks through intense heat and pressure. The rock is foliated and often has a high luster due to large crystals within the rock(Akintola, 1994).

## METHODOLOGY

2D electrical resistivity survey was employed using Wenner electrode array with -electrode spacing of 5m, 10m, and 15m and station increment of 5m along 5 traverses of lengthsranging from 85 m to 200 m (Fig. 3).The data were acquired with a resistivity meter and its accessories

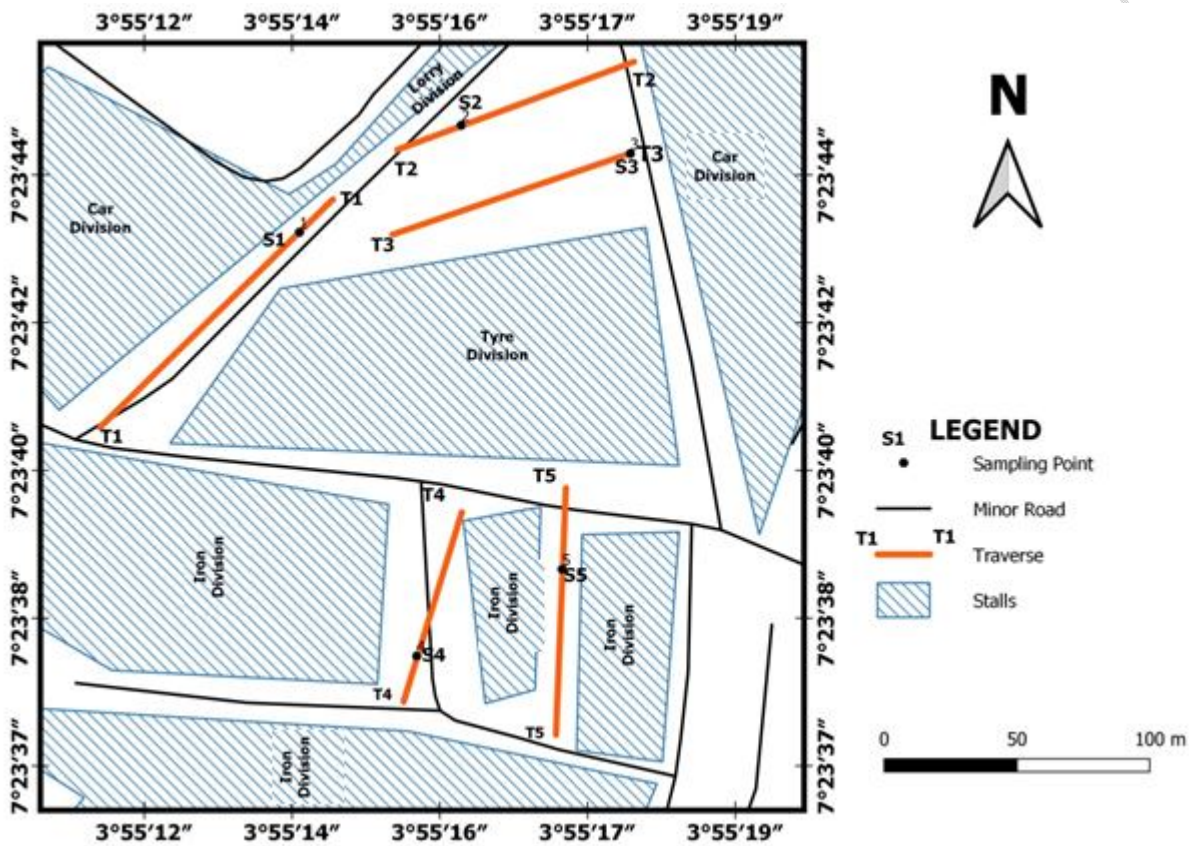


Fig. 3: Field layout of the geophysical traverses and soil sampling points

and processed by using 2D inversion procedure to generate the 2D inverted resistivity earth sections. The program used a forward modelling subroutine to calculate apparent resistivity values from field data, which were then inverted using a nonlinear least-squares optimization technique (Loke, 2010). Anomalous low resistivity zones indicating the mature hydrocarbon-contaminated soils were delineated on the 2D inverted resistivity sections.

Oil-stained soil samples were collected from test pits dug along the traverses to the depths of the observed resistivity lows. The samples were air-dried for 8 days in the laboratory, free of dust and chemical fumes. They were pulverized and 100g of each was measured into sample bottles.

Extraction was done in a sonicator using 40ml of dichloromethane for 40 minutes. The procedure was repeated three times.

The extract was obtained and kept in a clean dust-free laboratory for 12 days to enable vaporization of the solvents after which the concentrations of the polycyclic aromatic hydrocarbons (PAHs) in each sample was determined by using Gas Chromatography–Flame Ionization Detection(GC-FID). The total concentration of the PAHs in each sample was computed and used to classify the levels of contamination in the study area.

## RESULTS AND DISCUSSION

### 2D Resistivity Imaging

The 2D inverted resistivity sections beneath the Traverses run across the study area show subsurface heterogeneity with characteristic lateral and vertical resistivity variations. Mature hydrocarbon-contaminated zones are characterized by anomalous low resistivity values, generally less than 10  $\Omega\text{m}$ , indicating the presence of high ionic contents and increased conductivity resulting from biodegradation of the polycyclic aromatic hydrocarbons contained in the used motor oil.

Traverse 1 is underlain by clayey overburden whose resistivity ranges from 10.8  $\Omega\text{m}$  to 45.1  $\Omega\text{m}$  and weathered bedrock with resistivity varying from 64.1  $\Omega\text{m}$  to 282  $\Omega\text{m}$  (Fig. 4). The high resistivity values in the topsoil probably indicate contamination by used oil spillage. Resistivity of the bedrock ranges from 433  $\Omega\text{m}$  to 13971  $\Omega\text{m}$ . Depth to the bedrock is about 2 m.

The bedrock is fractured beneath stations 7 to 15, 21 to 27 and 31 to 36, providing pathways for the migration of contaminants through the rocks. Lowresistivity anomalies of values ranging from 1.85  $\Omega\text{m}$  to 12.5  $\Omega\text{m}$  occurring within the fractures at depths below 2.5 m suggest contamination plumes of mature hydrocarbons. Similar low resistivity values have been reported for mature hydrocarbons contaminated sites in previous studies such as Ehirimet *et al.*, 2016, Caterina *et al.* 2017 and Eze *et al.* 2021.

The 2D inverted resistivity section beneath Traverse 2 (Fig. 5) reveals overburden resistivity varying from 13.5  $\Omega\text{m}$  to 30.9  $\Omega\text{m}$  and bedrock resistivity ranging from 46.5  $\Omega\text{m}$  to 828  $\Omega\text{m}$  indicating intensely/fairly weathered bedrock. The bedrock is fractured beneath stations

6 to 10. The fracture hosts a zone of anomalously low resistivity (2.42 Ωm – 5.54 Ωm) from about 2.5 m depth downwards, representing suspected mature hydrocarbon contamination. The resistivity lows

Traverse 1 (2-D Resistivity Structure)

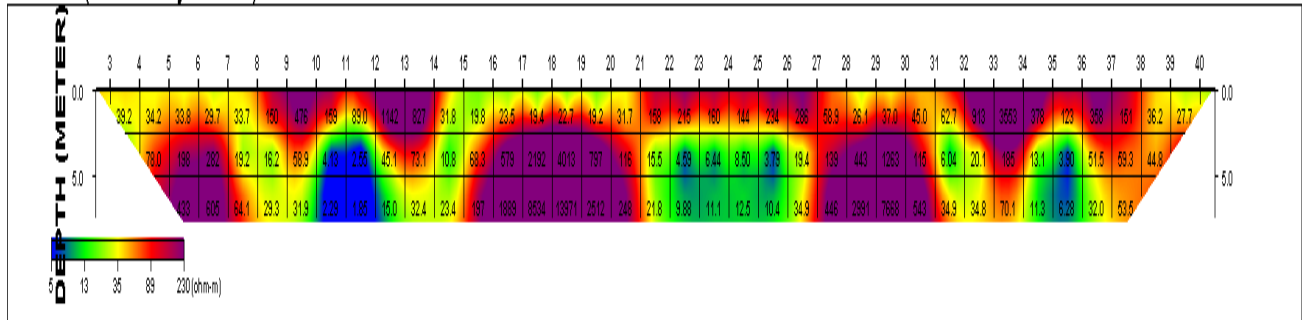


Fig.4: 2D inverted resistivity section beneath Traverse 1

Traverse 2 (2-D Resistivity Structure)

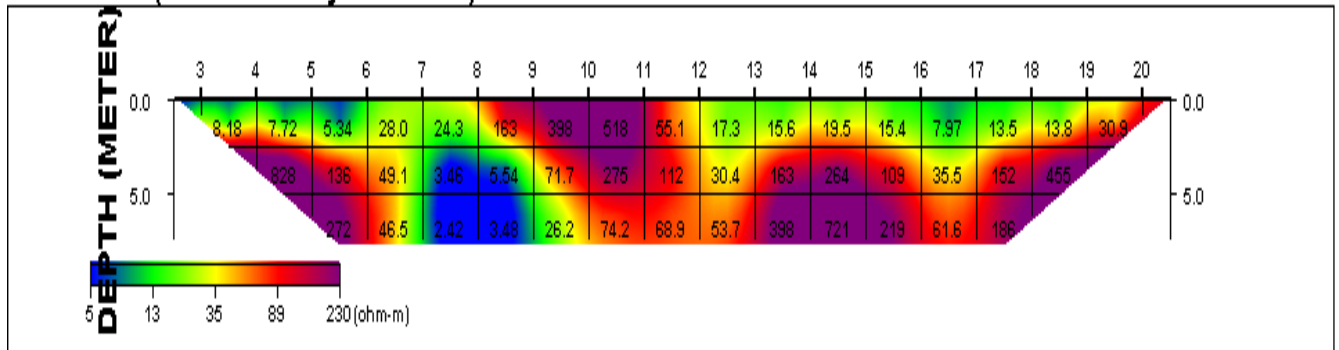


Fig. 5: 2D inverted resistivity section beneath Traverse 2

beneath stations 1 to 6 and stations 16-17 may be due to uncontrollably disposed pieces of waste metallic substances buried over time within the topsoil. The zone of relatively high resistivity (163 Ωm – 518 Ωm) beneath stations 9 to 11, from surface to about 4 m, probably suggests contamination by used hydrocarbons not yet biodegraded.

The resistivity distribution beneath Traverse 3 delineate overburden resistivity ranging from 14.7 Ωm to 89.6 Ωm typical of clay (Fig. 6). The relatively higher resistivity (196 Ωm – 242 Ωm) beneath stations 6 to 7 may be due to fresh contamination by used oil spillage while the resistivity

lows (2.62  $\Omega\text{m}$  – 6.35  $\Omega\text{m}$ ) beneath stations 18 to 20 possibly indicate buried pieces of uncontrollably disposed waste metallic substances. The resistivity of the bedrock (132  $\Omega\text{m}$  – 544  $\Omega\text{m}$ ) suggests intense weathering. Depth of the bedrock is about 3 m and it outcrops between

### Traverse 3 (2-D Resistivity Structure)

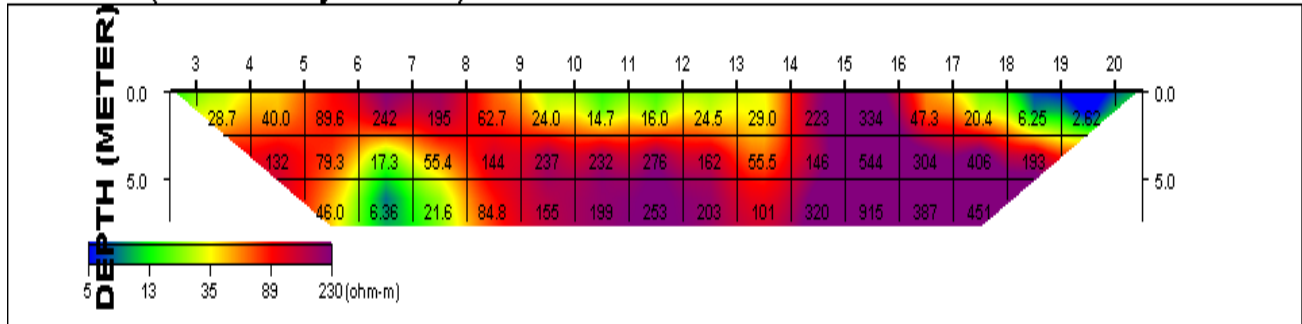


Fig. 6: 2D inverted resistivity section beneath Traverse 3

stations 14 and 16. The bedrock is fractured beneath stations 6 to 8 and indicates anomalous resistivity low zones suspected to be contamination plume of mature biodegraded hydrocarbons.

The 2D inverted resistivity section beneath Traverse 4 depicts clayey overburden with resistivity ranging from 11.0  $\Omega\text{m}$  to 105  $\Omega\text{m}$  (Fig. 7). The resistivity lows (4.33  $\Omega\text{m}$  – 7.48  $\Omega\text{m}$ ) beneath stations 10 – 12 may be due to buried pieces of uncontrollably disposed waste metallic substances. Resistivity of the bedrock varies from 149  $\Omega\text{m}$  to 5031  $\Omega\text{m}$  representing weathered /fresh bedrock. The bedrock is fractured beneath stations 6-8 and 13-14 while the resistivity lows (1.53  $\Omega\text{m}$  – 4.02  $\Omega\text{m}$ ) occurring in the depth interval 2.5 m – 5.0 m possibly delineate contamination plumes of mature biodegraded hydrocarbons.

The resistivity of the overburden beneath Traverse 5 ranges from 11.1  $\Omega\text{m}$  to 77.3  $\Omega\text{m}$  characteristic of clay (Fig. 8). The bedrock has resistivity varying from 149  $\Omega\text{m}$  to 3454  $\Omega\text{m}$  representing weathered/fresh bedrock. Its outcrop occurs between station 5 and station 8 while it is fractured from station 7 to station 11. The resistivity lows (2.98  $\Omega\text{m}$  - 4.24  $\Omega\text{m}$ ) below 3 m depth within the fracture suggest contamination plume of mature, biodegraded hydrocarbons.

### Traverse 4 (2-D Resistivity Structure)

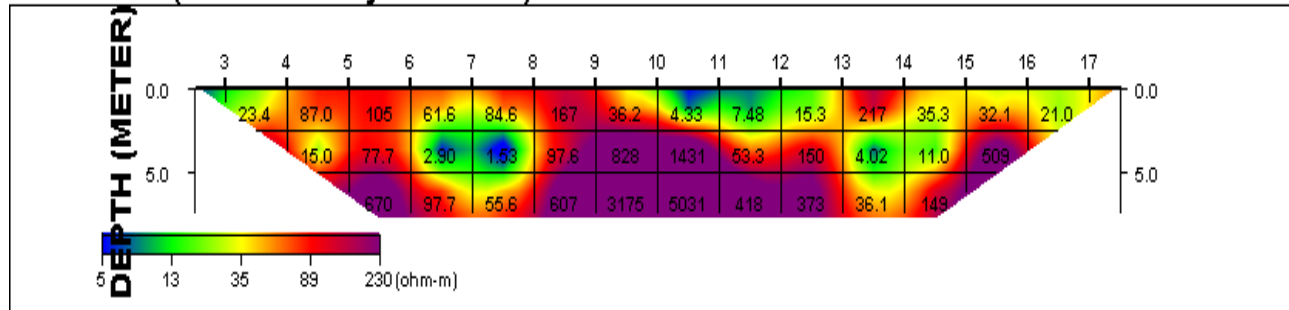


Fig. 7:2D inverted resistivity section beneath Traverse 4

### Traverse 5 (2-D Resistivity Structure)

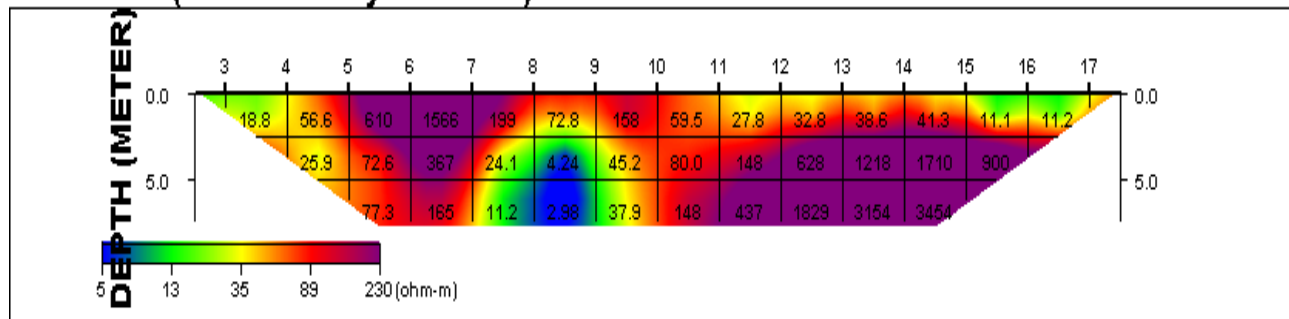


Fig. 8:2D inverted resistivity section beneath Traverse 5

### Geochemical analysis of soil samples for Polycyclic Aromatic Hydrocarbons

The concentrations (in  $\mu\text{g}/\text{kg}$ ) of the 17 PAHs extracted from the soils studied are presented in Table 1. The total concentration of PAHs ranges from 1390.4  $\mu\text{g}/\text{kg}$  in Sample 4 to 16140.03  $\mu\text{g}/\text{kg}$  in Sample 2. The high molecular weight PAHs (HPAHs) are the main contributors accounting for about 86.28% to 95.79% of the total PAHs in the soils. This indicates that the PAHs are of combustion origin. HPAH/LPAH ratio greater than 1 typically indicates pyrogenic (combustion) origin while HPAH/LPAH ratio less than 1 indicates petrogenic (fresh liquid fuels) source (Havelcova *et al.*, 2014; Emoyan *et al.*, 2015b, Adeyeni *et al.*, 2016).

This claim is also supported by the diagnostic ratios Phe/Ant less than 10 and Flu/Pyr greater than 1 obtained for the study area (Wanget *et al.*, 2014, Lawal and Fantke, 2017). Composition of the low molecular weight PAH(LPAH) ranges from 4.21% in Sample 2 to 13.72% in Sample 4. HPAHs are generally hydrophobic and partition more readily into organic matter than LPAHs (Chai *et al.*, 2022).

Name of PAHs	No. of Rings	Sample 1(μg/kg)	Sample 2(μg/kg)	Sample 3(μg/kg)	Sample 4(μg/kg)	Sample 5(μg/kg)
Naphthalene Nap	2	-	12.95	20.76	26.97	32.08
Acenaphthylene Acy	3	2.74	53.38	28.42	44.44	8.56
AcenaphtheneAcp	3	21.17	33.00	24.27	15.17	14.49
Fluorene, Flr	3	6.03	334.80	177.92	80.78	152.31
Phenanthrene, Phe	3	45.43	173.72	69.04	1091.60	63.55
Anthracene, Ant	3	7.59	70.82	3.29	52.51	7.30
Fluoranthene Flt	4	9.63	1546.10	594.43	9.79	39.51
Pyrene, Pyr	4	4.61	333.11	21.96	38.26	26.04
Benzo[c]phenanthreneBcPh	4	3.33	792.53	347.18	349.29	14.45
Benzo[a]anthraceneBaA	4	202.54	4038.12	1667.10	172.81	141.45
Chrysene Chr	4	3.48	1134.77	435.57	553.73	15.10
Benzo[j+k+b]fluoranthene	5	17.16	438.94	152.28	197.42	154.67
Benzo[e]pyrene	5	200.54	148.96	140.82	1745.81	257.05
Benzo[a]pyreneBaP	5	32.02	83.18	217.19	26.28	465.82
Benzo[g,h,i]peryleneBghiP	6	97.04	189.16	77.18	626.34	884.03
Indeno[1,2,3,-cd]pyreneIcP	6	546.06	6083.86	199.49	1071.93	582.95
Dibenz[a,e]pyrene DeP	6	191.03	672.63	226.45	3453.42	16.04
%LPAHs		5.97	4.21	7.35	13.72	9.68
%HPAHs		94.03	95.79	92.65	86.28	90.32
Carcinogenic PAHs		801.26	11778.87	2671.63	2022.17	1359.99
Total PAHs Conc.(Σ17PAHs)		1390.40	16140.03	4403.35	9556.55	2875.40

Table 1: PAH Concentrations in soil samples from the study area

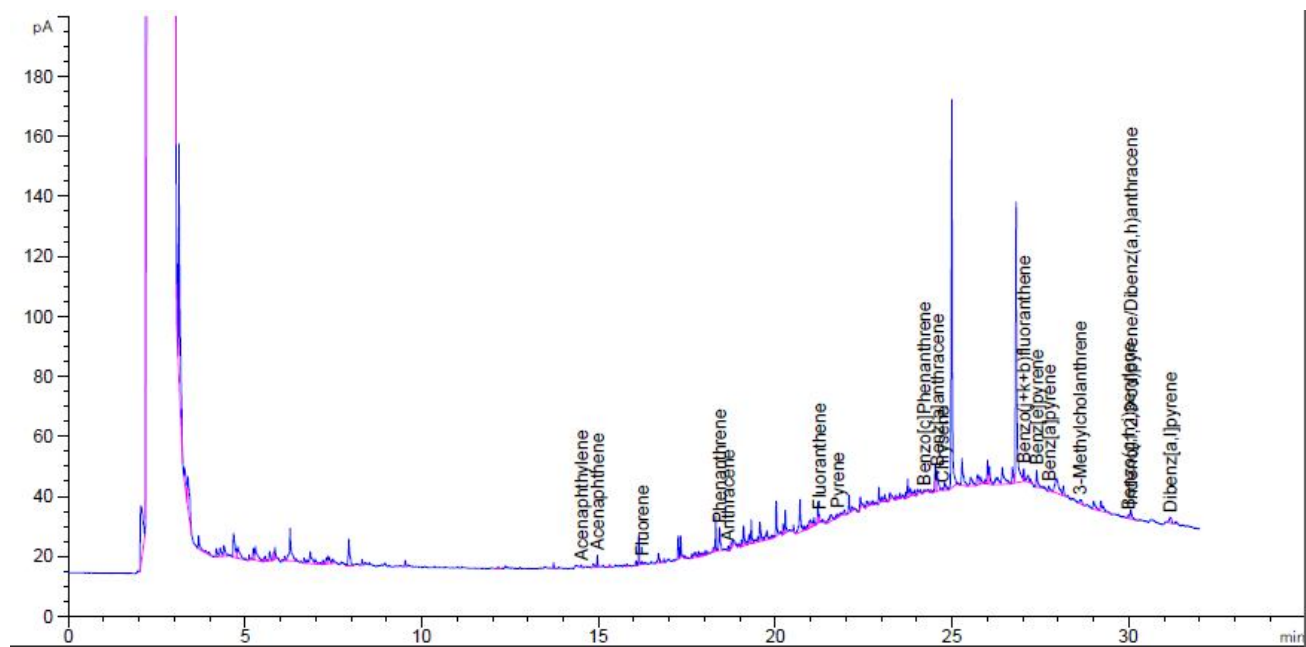


Fig. 9: Typical GC-FID Chromatogram of PAH concentrations in soil samples from the study area

Typical GC-FID Total Ion Chromatogram which shows the concentrations of the different PAHs in the soil samples is presented in Fig. 9. The PAHs are distinguished by the different hydrocarbon fingerprints that they exhibit in the chromatograms. In accordance with the European Classification System of Soil Contamination in which total concentration of PAHs,  $\Sigma$ PAHs < 200  $\mu\text{g}/\text{kg}$  indicates no contamination, 200–600  $\mu\text{g}/\text{kg}$  corresponds to weak contamination, 600–1000  $\mu\text{g}/\text{kg}$  represents moderate contamination, and >1000  $\mu\text{g}/\text{kg}$  suggests heavy contamination (Maliszewska-Kordybach, 1996), the study area is highly contaminated (Table 2).

The total PAHs concentrations for Sample 1 to Sample 5 are respectively 1.39, 16.14, 4.403, 9.557 and 2.875 times higher than the heavily contaminated level of 1000  $\mu\text{g}/\text{kg}$ . The dominant PAH in Sample 1 and Sample 2 is Indeno[1,2,3-cd]pyrene with concentrations of 546.06  $\mu\text{g}/\text{kg}$  and 6083.86  $\mu\text{g}/\text{kg}$  representing 39.27% and 37.69% of the total concentration respectively. Benzo[a]anthracene is the predominant PAH in Sample 3 at 1667.1  $\mu\text{g}/\text{kg}$ , and is notably present next to Indeno[1,2,3-cd]pyrene in Sample 1 at 202.54  $\mu\text{g}/\text{kg}$  and Sample 2 at 4038.12  $\mu\text{g}/\text{kg}$ . The most abundant PAH in Sample 4 is Dibenz[a,c]pyrene at 3453.42  $\mu\text{g}/\text{kg}$  while the

highest concentration in Sample 5 is Benzo[g,h,i] perylene at 884.03  $\mu\text{g}/\text{kg}$  followed by Indeno[1,2,3,-cd] pyrene (582.95  $\mu\text{g}/\text{kg}$ ) and Benz [a] pyrene (465.82  $\mu\text{g}/\text{kg}$ ).

Table 2: Classification of contamination level of soil samples from the study area (based on Maliszewska-Kordybach 1996)

Sample No.	Total Concentration ( $\mu\text{g}/\text{kg}$ )	Contamination level
Sample 1	1390.4	Heavily contaminated
Sample 2	16140.03	Heavily contaminated
Sample 3	4403.35	Heavily contaminated
Sample 4	9556.55	Heavily contaminated
Sample 5	2875.4	Heavily contaminated

The International Agency for Research on Cancer (IARC) and the United State Environment Programme, (USEPA) listed chrysenene, benzo(a)anthracene, dibenzo(a,h)anthracene, benzo(a)pyrene, benzo(b)fluoranthrene, benzo(k)fluoranthrene and indeo(1,2,3-cd)pyrene as the topmost potential human carcinogens. Dibenzo(a,h)anthracene was not detected in the soils from the study area. The total concentration of carcinogenic PAHs ranges from 801.26 $\mu\text{g}/\text{kg}$  in Sample 1 to 11778.87  $\mu\text{g}/\text{kg}$  in Sample 2. These carcinogens and the others detected in the study area constitute potential health risk to all forms of life by contact via breathing and ingestion.

This study has shown that the subsoils have been impacted by large amounts of PAHs. The PAHs resulted mostly from pyrogenic sources. Remedial measures are necessary to clean the area prevent further spread into neighbouring soil and groundwater systems. The results are expected to serve as useful guide in planning remediation programme for the area and its vicinity.

## CONCLUSIONS

The study has demonstrated the effectiveness of combining 2D electrical resistivity imaging with geochemical analysis in characterizing hydrocarbon-contaminated sites. The low resistivity

anomalies delineated on the 2D resistivity sections revealed mature biodegraded hydrocarbon contamination. The results of geochemical analysis indicated that the study area is highly contaminated by the used motor oil and may constitute potential health risk to the soil and groundwater systems in its vicinity.

## REFERENCES

- Abass, M., Jardani, A. A., Machour, N. and Dupoit, J. P., 2018. Geophysical and geochemical characterisation of a site impacted by hydrocarbon contamination undergoing biodegradation. *Near Surface Geophysics* 16(2):176-192.
- Adeniji, A. O., Okoh, O. O. and Okoh, A.I., 2019. Levels of polycyclic aromatic hydrocarbons in the water and sediment of Buffalo River estuary, South Africa and their health risk assessment. *Arch. Environ. Contam. Toxicol.*, 76, p. 657-669.
- Adeyeni, E. G., Adedosu, T. A., Bello, O. S., Adedosu, H. O., Adeniyi, T. A., Awoyemi, T. N., 2016. Evaluation of Polycyclic Aromatic Hydrocarbons in SOIL within the vicinity of an Industrial Estate, Sango Otta, Nigeria. *J. Chem. Soc. Nigeria*, Vol. 41, No. 1, p. 117-124.
- Akinrinade, O.J., Oladapo, M. I. and Christopher, O., 2016. Geoelectric delineation of hydrocarbon spill in Abesan Lagos, Nigeria. *Journal of Emerging Trends in Engineering and Applied Sciences*, 7(1), 35-44.
- Akintola F.O, 1994. Geology and hydrology of the Ibadan region. [in:] Filani, M.O., Akintola, F. O., Ikporukpo C. (eds.), Ibadan Region. Chapter 3, Rex Charles Pub., Nigeria: 1827.
- Ambade, B.; Sethi, S.S., 2021. Health risk assessment and characterization of polycyclic aromatic hydrocarbon from the hydrosphere. *J. Hazard. Toxic Radioact. Waste* 2021, 25.
- Arato, A., Wehrer, M., Biró, B. and Godio, A., 2014. Integration of geophysical, geochemical and microbiological data for a comprehensive small-scale characterization of an aged LNAPL-contaminated site *Environ Sci Pollut Res.* 21:8948–8963.
- Azahar, M.A., Suryadi, A., Samsudin, A.R., Yaacob, W.Z.W. and Saidin, A.N., 2016. 2D Geoelectrical resistivity imaging (ERI) of hydrocarbon contaminated soil. *Electronic Journal of Geotechnical Engineering*, 21, 299-304.
- Balmer, J. E., Hung, H., Yu, Y., Letcher, R. J. and Muir, R. C, 2019. Sources and environmental fate of pyrogenic polycyclic aromatic hydrocarbons (PAHs) in the Arctic, *Emerging Contaminants*, 5 (2019), pp. 128-142.
- Bertolla L, Porsani J.L, Soldovieri F, Catapano I., 2014. GPR-4D monitoring a controlled LNAPL spill in a masonry tank at USP, Brazil. *J Appl Geophys* 103:237–244.
- Caterina, D., Flores-Orozco, A., Nguyen F., 2017. Long-term ERT monitoring of biogeochemical

changes of an aged hydrocarbon contamination. *J ContamHydrol* 201:19–29.

Chai G., Dongqi W., Shan J., Jiang C., Zhangjie Yang, Z., Liu E., Meng H., Wang H., Wang Z., Qin L., Jiayao J., Ma Y., Li H., Qian Y., Li J., Lin Y., 2022. Accumulation of high-molecular-weight polycyclic aromatic hydrocarbon impacted the performance and microbial ecology of bioretention systems. *Chemosphere*, Vol. 298, 134314.

Ciampi, P., Esposito, C., Cassiani, G., Deidda, G. P., Flores-Orozco, A., Rizzetto, P., Chiappa, A., Bernabei, M., Gardon, A., Papini, M. P., 2022. Contamination presence and dynamics at a polluted site: Spatial analysis of integrated data and joint conceptual modeling approach. *Journal of Contaminant Hydrology*, Vol. 248, 104026.

Delgado-Rodríguez, O., Shevnin, V., Peinado-Guevara, H. and de Guevara-Torres, M.L., 2018. Characterization of hydrocarbon-contaminated sites based on geoelectrical methods of geophysical exploration. In: A. Okiwelu, ed. *Geophysics*. London: InTechOpen, p. 85-93.

Egbinola, C.N. and Amanambu, C.A., 2013, Climate variation assessment based on rainfall and temperature in Ibadan, South-Western, Nigeria. *Journal of Environment and Earth Sciences*, 3: 32–45.

Ehirim, C. N., Adizua, O. F. and Okorie, I. P. C., 2016. Geoelectrical Characterization of Matured Petroleum Hydrocarbon impacted soil in Port Harcourt, Nigeria. *Asaian Journal of Earth Sciences*, 9: 9-15.

Eldos, H. I., Ashfaq, M. Y. and Al-Ghouti, M. A., 2020. Rapid assessment of the impact of microwave heating coupled with UV-C radiation on the degradation of PAHs from contaminated soil using FTIR and multivariate analysis *Arabian J. Chem.*, 13 (11), p. 7609-7625.

Emoyan O. O., Agbaire. P. O., S.O. Akporido, S. O., Variability in polycyclic aromatic hydrocarbons (PAHs) isomer pair ratio: source identification concern, *Int. J. Environ. Monit. Anal.* 3 (3) (2015b) 111–117.

Eze, S. U., Ogagarue, D. O., Nnorom, S. L., Osung, W. E., Ibitoye, T. A., 2021. Integrated Geophysical and Geochemical Methods for Environmental Assessment of Subsurface Hydrocarbon Contamination. *Environmental Monitoring and Assessment* 193 (7), 193-451.

Faboya, L. O. Sojinu, S. O. and Otugboyega, J. O., 2023. Preliminary investigation of polycyclic aromatic hydrocarbons (PAHs) concentration, compositional pattern, and ecological risk in crude oil-impacted soil from Niger delta, Nigeria, *Heliyon*, 9, p.1-10.

Havelcova, M., Meleg. A., Rapant, S., 2014. Geochemical distribution of polycyclic aromatic hydrocarbons in soils and sediments of El-Tabbin, Egypt. *Chemosphere* 95: 63–74.

Koroma, S., Arato, A. and Godio, A., 2015. Analyzing geophysical signature of a hydrocarbon-contaminated soil using geoelectrical surveys. *Environmental Earth Sciences* 74(4):2937-2948.

Lawal, A. T., and Fantke, P., 2017. Polycyclic aromatic hydrocarbons. A review. *Cogent Environmental Science*, 3(1). <https://doi.org/10.1080/23311843.2017.1339841>.

Loke, M.H., 2010. *Rapid 2D Resistivity & IP Inversion Using Least-Squares Method*; Tutorial Geotomo Software: Penang, Malaysia.

Maliszewska-Kordybach, B., 1996. Polycyclic aromatic hydrocarbons in agricultural soils in Poland: Preliminary proposals for criteria to evaluate the level of soil contamination. *Applied Geochemistry*, Volume 11, Issues 1–2, p. 121-127.

Omole, E.O, Ikokide, S.Y. and Adeyemi, S.O., 2021. Investigation into People's Awareness of Effect of Contaminated Groundwater in Araromi Spare Parts Market, Agodi Gate, Ibadan. *Journal of African Sustainable Development*, Vol. 28 (2), p. 249-262.

Orlando L, Renzi B., 2015. Electrical permittivity and resistivity timelapses of multi-phase DNAPLs in a lab test. *Water Resour. Res* 51: 377–389.

Oyinkuro, O.A. and Wariebi, K.A., 2017. Hydrocarbon spill site characterization by electrical resistivity tomography and ground penetrating radar methods - A review. *Asian Journal of Environment and Ecology*, 4(3), p. 1-9.

Power, C, Gerhard, J. I., Tsourlos, P., Soupios, P., Simyrdanis, K., Karaoulis, M., 2015. Improved time lapse electrical resistivity tomography monitoring of dense non-aqueous phase liquids with surface-to-horizontal borehole arrays. *J Appl Geophys* 112:1–13.

Rosales, R.M., Martínez-Pagán, P., Faz, A, Bech, J., 2014. Study of Subsoil in former Petrol Stations in SE of Spain: Physicochemical Characterization and Hydrocarbon Contamination Assessment. *J Geochem Explor.*, 147:306–320.

Ugochukwu, U. C. and Ochonogor, A., 2018. Groundwater contamination by polycyclic aromatic hydrocarbon due to diesel spill from a telecom base station in a Nigerian City: assessment of human health risk exposure. *Environmental Monitoring and Assessment* 190(4): 249.

Simyrdanis, K., Papadopoulos, N., Soupios, P, Kirkou, S., Tsourlos, P., 2018. Characterization and Monitoring of Subsurface Contamination from Olive Oil Mills' Waste waters using electrical resistivity. *Tomography Sci Total Environ* 637(638):991–1003.

Subba, R. C. and V. Chandrashekar, 2014, Detecting oil contamination by ground Penetrating Radar around an oil storage facility in Dhanbad, Jharkhand, India: *Journal of India Geophysical Union*, 18, 448–454.

Sun, K., Song, Y., He, F., Jing, M., Tang, J. and Liu, R., 2021. A review of human and animals' exposure to polycyclic aromatic hydrocarbons: Health risk and adverse effects, photo-induced toxicity and regulating effect of microplastics. *Sci. Total Environ.*, 773.

Wang, Z., Yang, C., Parrot, J. L., Yang, Z., Brown, C. E., Hollenbone, B.P., Landrail, M., Fieldhouse, B., Liu, Y., Zhan, G., Heiwilt, L. M., 2014. Forensic source identification of petrogenic, pyrogenic and biogenic hydrocarbon in the Canadian Oil Sands Environmental Sample. *Journal of Hazard Mater*, 271:166-177.

UNDER PEER REVIEW